ELSEVIER

Journal of Volcanology and Geothermal Research 101 (2000) 253–271

Journal of volcanology and geothermal research

www.elsevier.nl/locate/jvolgeores

Fluid flow from pore pressure measurements off La Palma, Canary Islands

R. Urgeles[a,*], M. Canals[a], J. Roberts[b,1] and the SNV "Las Palmas" Shipboard Party[2]

[a]*GRC Geociències Marines, Dept. d'Estratigrafia i Paleontologia, Facultat de Geologia, Universitat de Barcelona, Campus de Pedralbes, E-08071 Barcelona, Spain*

[b]*GEOTEK Ltd, Unit 3 Faraday Close, Drayton Fields, Daventry, Northamptonshire NN11 5RD, UK*

Received 13 August 1999; received in revised form 23 January 2000; accepted 23 January 2000

Abstract

In situ subseafloor pore pressure results from the western flank of the island of La Palma, Canary Islands, are presented. The data obtained with a Pop Up Pore Pressure Instrument (PUPPI) provide constraints on the fluid circulation and its causes in a very special context: The sediment piles near an intraplate oceanic island built on the continental rise of the Northwest African Margin. The ambient pore pressures estimated from 2 to 4 days long record are negative in almost all cases with values, at depths of a few meters below sea floor, usually on the order of −10 to −70 Pa. Excess pore pressures develop only in the distal most areas. The permeabilities and compressibilities obtained respectively from the decay of the insertion pressures and the amplitude of the tidally induced pore pressure variations range between 2.5×10^{-18} and 6.6×10^{-16} m^2 and, 6.2×10^{-9} and 1.5×10^{-7} Pa^{-1}. According to these permeabilities fluid flow is estimated to be mostly downward and usually on the range between 0 and −0.3 mm y^{-1}. However, from the excess pore pressure profile a complex pattern of fluid circulation is inferred where horizontal fluid motion cannot be neglected. Horizontal flow is probably controlled by significant contrasts in the permeability of the different layers. The prevailing downward fluid flow is abnormal for a classical passive margin. We thus interpret these results as the superposition to the loss of fluids by sediment compaction (on the continental rise), of a large-scale flow system stimulated by thermal buoyancy (100 km wide) related to the volcanic activity on the island of La Palma.

Keywords: pore pressure; piezometer; hydrothermal processes; Canary Islands

1. Introduction

In recent years in situ pore pressure measurements have been made in a wide variety of environments, such as ridge crests (Davis et al., 1991) and ridge flanks (Davis et al., 1986, 1991; Langseth et al., 1992; Fang et al., 1993), but also on river deltas (Hirst and Richards, 1976; Bennett et al., 1982), coastal areas (Bennett et al., 1996), deep lakes (Harvey et al., 1998) and abyssal plains (Schultheiss and Noel, 1987). These measurements have been mainly carried out to study hydrothermal circulation in the oceanic crust (e.g. Davis et al., 1991) or to estimate in situ geotechnical properties of marine sediments (e.g. Bennett et al., 1982). Little is known however of the role of pore pressure and fluid flow on

* Corresponding author. Tel.: + 34-3-4021369; fax: + 34-3-4021340.

E-mail addresses: roger@beagle.geo.ub.es (R. Urgeles); miquel@natura.geo.ub.es (M. Canals); roberts@geotek.co.uk (J. Roberts).

[1] Tel.: + 44-1327-31166; fax: + 44-1327-311555.

[2] SNV "Las Palmas" Shipboard Party: Belén Alonso, Ignacio Alonso, Jesus Baraza and Peter Schultheiss.

0377-0273/00/$ - see front matter
PII: S0377-0273(00)00176-1

Nomenclature

A_c	Correction for anisotropic consolidation (dimensionless)
A_r	Correction for cyclic loading (dimensionless)
α	Slope angle (°)
β_f	Compressibility of the pore fluid (Pa^{-1})
g	Acceleration due to gravity ($m\ s^{-2}$)
γ	Total wet sediment unit weight (ρg) ($N\ m^{-3}$)
γ'	Effective sediment unit weight ($\gamma - \gamma_w$) ($N\ m^{-3}$)
γ_w	Unit weight of seawater ($N\ m^{-3}$)
k	Fraction of g (critical earthquake acceleration) required for sediment failure (dimensionless)
K	Permeability (m^2)
m	Sediment parameter typically about 0.8 (dimensionless)
m_v	Confined frame compressibility (Pa^{-1})
n	Fractional porosity (dimensionless)
μ	Viscosity of seawater (Pa s)
OCR	Overconsolidation ratio (dimensionless)
Q	Amplitude of the seafloor pressure variation (Pa)
S	Normalised strength parameter (dimensionless)
S_u	Shear strength (Pa)
σ'_v	Overburden pressure (Pa)
σ'_{vm}	Past overburden pressure (Pa)
U	Ratio σ'_v to $\gamma' z$(dimensionless)
u_{max}	Maximum insertion pressure (Pa)
u_e	Ambient equilibrium pore pressure (Pa)
u_t	Amplitude of the tidally induced pore pressure variations (Pa)
t_{50}	Half decay time (s)
τ_{50}	Dimensionless time factor for pore pressure to fall to 50% of its initial value (dimensionless)
v	Seepage velocity ($m\ s^{-1}$)
z	Depth in sediment (m)

deep-sea sediment accumulations adjacent to hot spot oceanic islands. In the Hawaiian chain, for instance, significant rates of hydrothermal fluid flow have been hypothesised (Garven and McNutt, 1995) in order to explain the apparent lack of a heat flow anomaly over the Hawaiian flexural moat (Von Herzen et al., 1989).

A special situation exists where intraplate oceanic islands develop over or near a passive margin, as in the region of the Canary Islands—NW African Margin. The sediment piles that accumulate on the continental margin can be thick enough to heat organic constituents and produce oil and gas. Fluid flow would, in principle, occur upwards as a result of positive buoyancy of these products and by compaction of the thick layers of sediment (Working Group 3, 1987). It should also be expected that the load associated with massive volcanoes, as is the case in the study area, would further compact the sediments and promote dewatering and upward fluid flow.

The pore pressure is also an important soil parameter that can only be measured in situ (Baligh, 1986; Schultheiss, 1990a), and which has a fundamental effect on the stability of sediments (Bea et al., 1975; Bennett et al., 1982; Schultheiss, 1990a). Over-pressured sediments will have lower shear strength and will therefore be less stable as the effective stress is thereby reduced.

In November–December, 1995 and May–June, 1996 two cruises were carried out on board the RRS *Discovery* and the SNV *Las Palmas*. During these cruises eleven Pop Up Pore Pressure Instruments (PUPPI) were deployed on the western reaches of

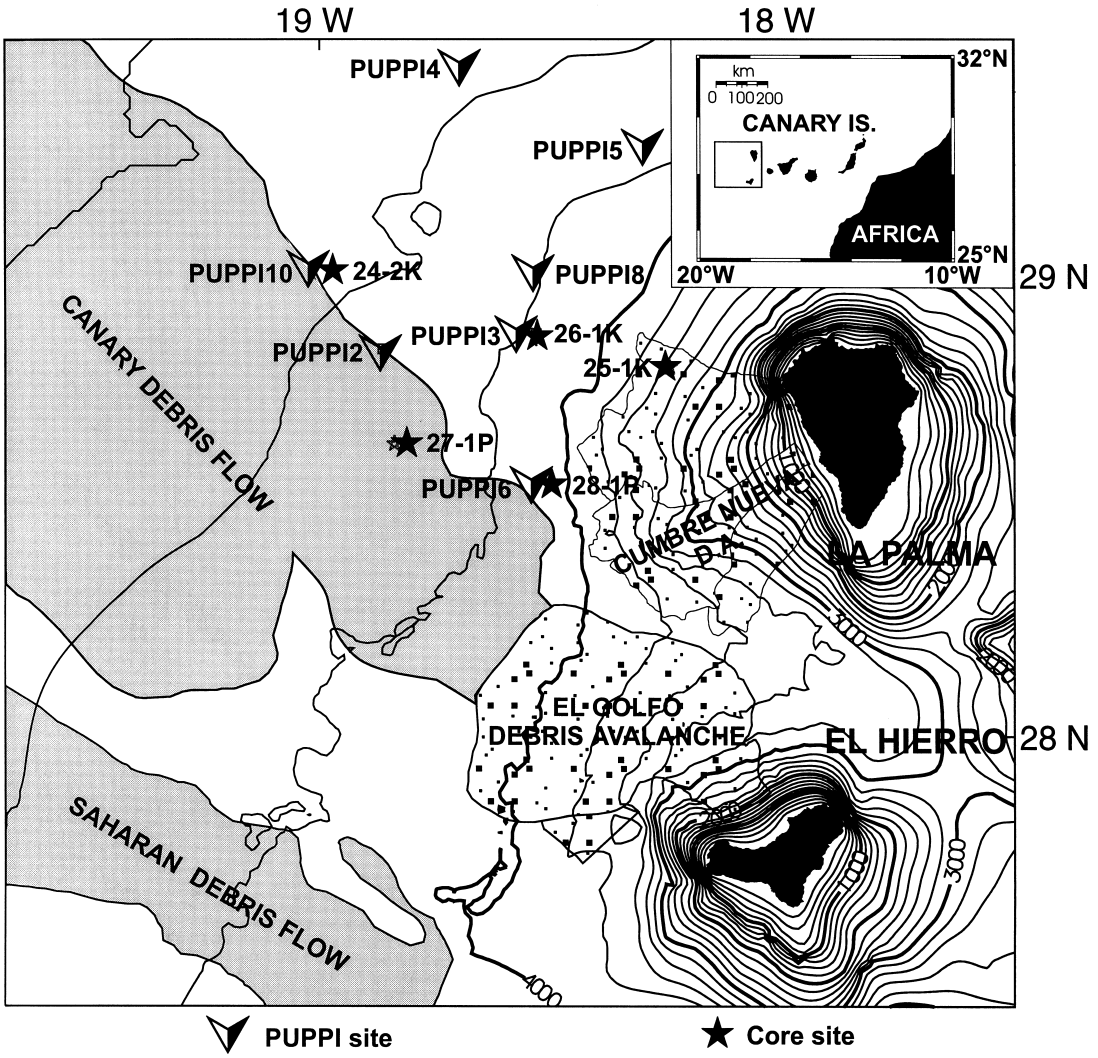

Fig. 1. Bathymetry of the study area and schematic facies mapping (modified from Masson, 1996; Urgeles et al., 1997; Urgeles et al., 1999) with the location of the PUPPI deployments, and cores discussed in Roberts and Cramp (1996). Contour interval is 200 m

La Palma between 4000 and 4500 m water depth. Six of the PUPPIs provided useful high-resolution records of the in situ pore pressure of sediment north of a large debris flow known as the Canary Debris Flow (Fig. 1, Table 1).

The objective of this study is to quantify the fluid flow through the seafloor sediments west of La Palma in order to better understand the hydrodynamic fluid circulation near ocean islands. Hydrothermal flow may induce abnormal pore water pressures in the flanks of the islands that may enhance, in turn, volcanic landslides. This process may be relevant on the island of La Palma, where the southern volcanic ridge is thought to be at the early stage of giant landslide initiation (Bonelli Rubio, 1950; Carracedo, 1994). It is also proposed that estimates of “in situ” properties from the piezometer data, such as pore water pressure and shear strength, will also allow to assess the role of these properties in sediment stability west of the island.

Table 1
PUPPI deployment data summary

Station number	Latitude (N)	Longitude (W)	Water depth (m)	Nearby core	Sediment field
PUPPI 2	28°50′	18°51.9′	4350		Undisturbed sediment on the northeastern edge of the Canary Debris Flow (CDF)
PUPPI 3	28°52.075′	18°32.142′	4110	CD56-26	Downslope side of sediment wave
PUPPI 4	29°25.647′	18°42.02′	4400		Downslope end of a sediment wave
PUPPI 5	29°14.958′	18°18.471′	4125		Sediment wave
PUPPI 6	28°33.1′	18°31.3′	4075	CD56-28	Undisturbed sediment on the eastern edge of the CDF
PUPPI 10	28°59.92′	19°00.02′	4410	CD56-24	Undisturbed sediment on the northeastern edge of the CDF

2. Geological setting

The Canary Islands form a ~500-km-long volcanic lineament of oceanic islands seaward of the Northwest African Margin. The islands are built over the continental slope and rise and hold a large history of volcanic activity expanding at least, from the Middle Miocene to present day (Hoernle and Schmincke, 1993). Seismic reflection studies west of the islands of La Palma and El Hierro suggest that the top of the oceanic basement is buried beneath 1 to 2 km of sediment (Ranero et al., 1995), with the lower values close to the islands (Urgeles et al., 1998). These studies suggest that there exists a depth-to-basement anomaly which is estimated to be about 500 m after correction for sediment loading (Ranero et al., 1995). In addition, gravity modelling indicates a lithospheric thinning in the vicinities of El Hierro and La Palma which has been interpreted as a sign of reheating of the old Mesozoic lithosphere beneath the Canary Basin (Ranero et al., 1995). The data of Urgeles et al. (1998) suggest that the sediments in the area where the PUPPIs were deployed is mainly made of silty volcaniclastic turbidites with interbedded hemipelagites.

The Canary Islands have been reported to suffer from large lateral collapses which affect both the subaerial and submarine slopes of the islands (Holcomb and Searle, 1991; Ancochea et al., 1994; Masson, 1996; Watts and Masson, 1996; Teide Group, 1997; Urgeles et al., 1997, 1999). These lateral collapses generate large debris avalanches that deposit on the lower slopes of the islands, thereby loading the hemipelagic sediments and triggering, in turn, huge debris flows and turbidity currents (Masson, 1996; Roberts and Cramp, 1996; Masson et al., 1998).

West of the islands of La Palma and El Hierro, several studies have been carried out in order to characterise the sedimentary processes and resulting deposits (Kidd et al., 1985; Simm et al., 1991; Masson et al., 1992; Masson, 1996; Urgeles et al., 1997; Masson et al., 1998). These include using a variety of mapping techniques such as deep-towed high-resolution side-scan sonar (TOBI), swath bathymetry and high- and ultrahigh-resolution seismic reflection profiling. These data have been validated by coring at different sites and geotechnical studies have been carried out on core samples to assess slope stability west of El Hierro and La Palma (Roberts and Cramp, 1996).

The most striking feature shown by those studies is the Canary Debris Flow (Masson, 1996), which develops immediately west and downslope of debris avalanche lobes in the western flanks of both islands (Masson, 1996; Urgeles et al., 1999) (Fig. 1). The single debris avalanche resulting from the collapse of the northern flank of the island of El Hierro and the Canary Debris Flow are two closely related events dated at about 15 ka (Masson, 1996) and have been estimated to account for a total volume of 580 km^3 (Masson et al., 1992; Urgeles et al., 1997).

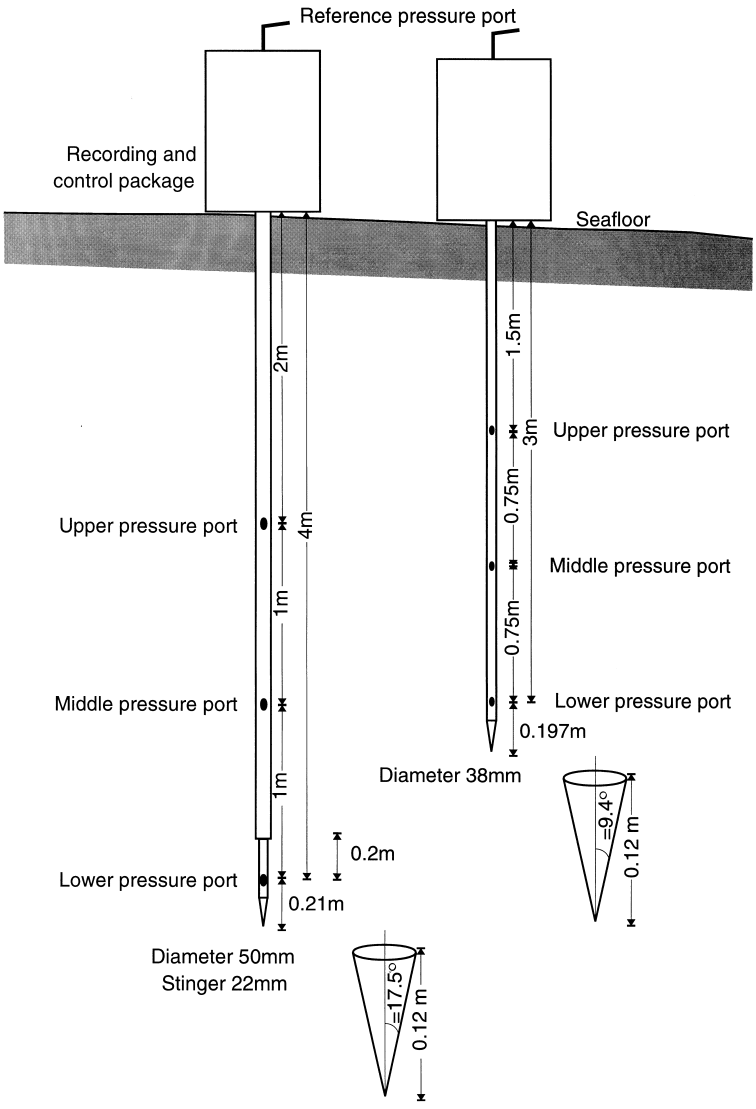

Fig. 2. Technical characteristics and dimensions of the PUPPI apparatus.

3. Methods

3.1. Pore pressure measurements

The Pop Up Pore Pressure Instrument (PUPPI) (Fig. 2), originally developed at the Institute of Oceanographic Sciences (Schultheiss and McPhail, 1986; Schultheiss and Noel, 1987), is designed and constructed to make accurate in situ measurements of the vertical pore pressure gradient in the seafloor. The PUPPI measures differential pore pressures at ports on a lance, with a resolution of about 5 Pa. It is a free-fall instrument that can be ballasted with lead or steel weights to penetrate a range of sediment types in water depths of up to 6000 m. The length of lance that can be used depends on the sediment stiffness. Typically a 4-m lance can be used successfully in soft hemipelagic sediments, although 6-m-long lances have also been used with success in deep-sea pelagic muds. During our cruises we used two types of PUPPI

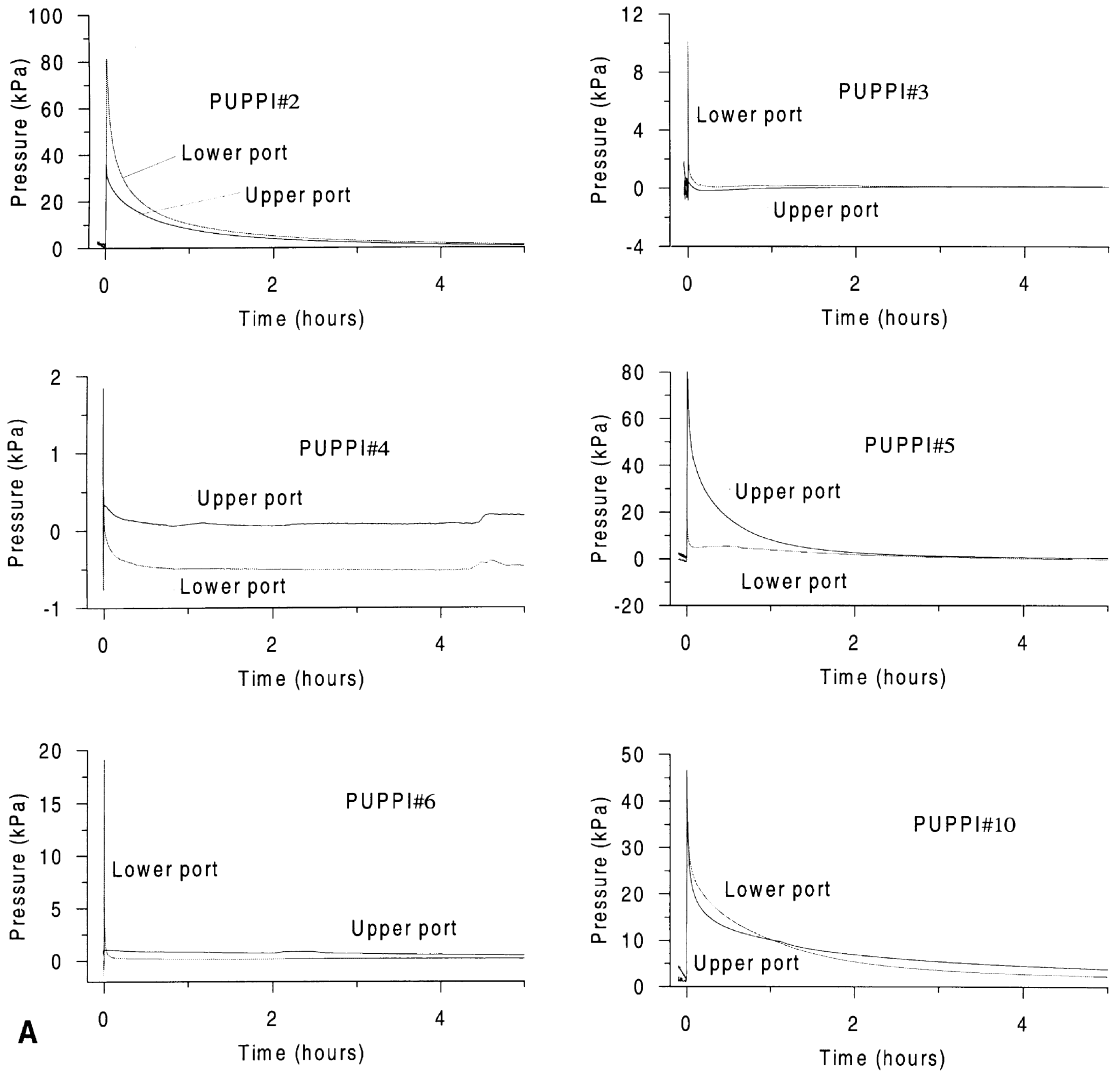

Fig. 3. Record of all PUPPI deployments where the initial high insertion pressures (A) and decay to ambient pore pressures with superimposed tidal cycles (B) can be observed.

lances with ports at 2, 3 and 4 mbsf and 1.5, 2.25 and 3 mbsf, respectively (Fig. 2). The probes were left on the sea floor for a period ranging from 50 to 90 h until insertion pressures were dissipated (Fig. 3).

Pore pressures are measured relative to hydrostatic at the porous ports on the lance using specially designed differential pressure transducers connected to the pressure ports and the open sea water. A microprocessor based data logger is used to record the data. Sampling rates are pre-programmed being normally rapid during the early part of the deployment (insertion and initial decay) but need only to be slow during the later stages when pressures only are changing slowly.

Whilst it is possible to calibrate the transducers for temperature and absolute pressure with a reasonable degree of accuracy, they cannot be calibrated for mechanical creep effects. These may be significant as the transducers are cycled through important changes in absolute pressure. Consequently, during our cruise a new motorised valve was used, which

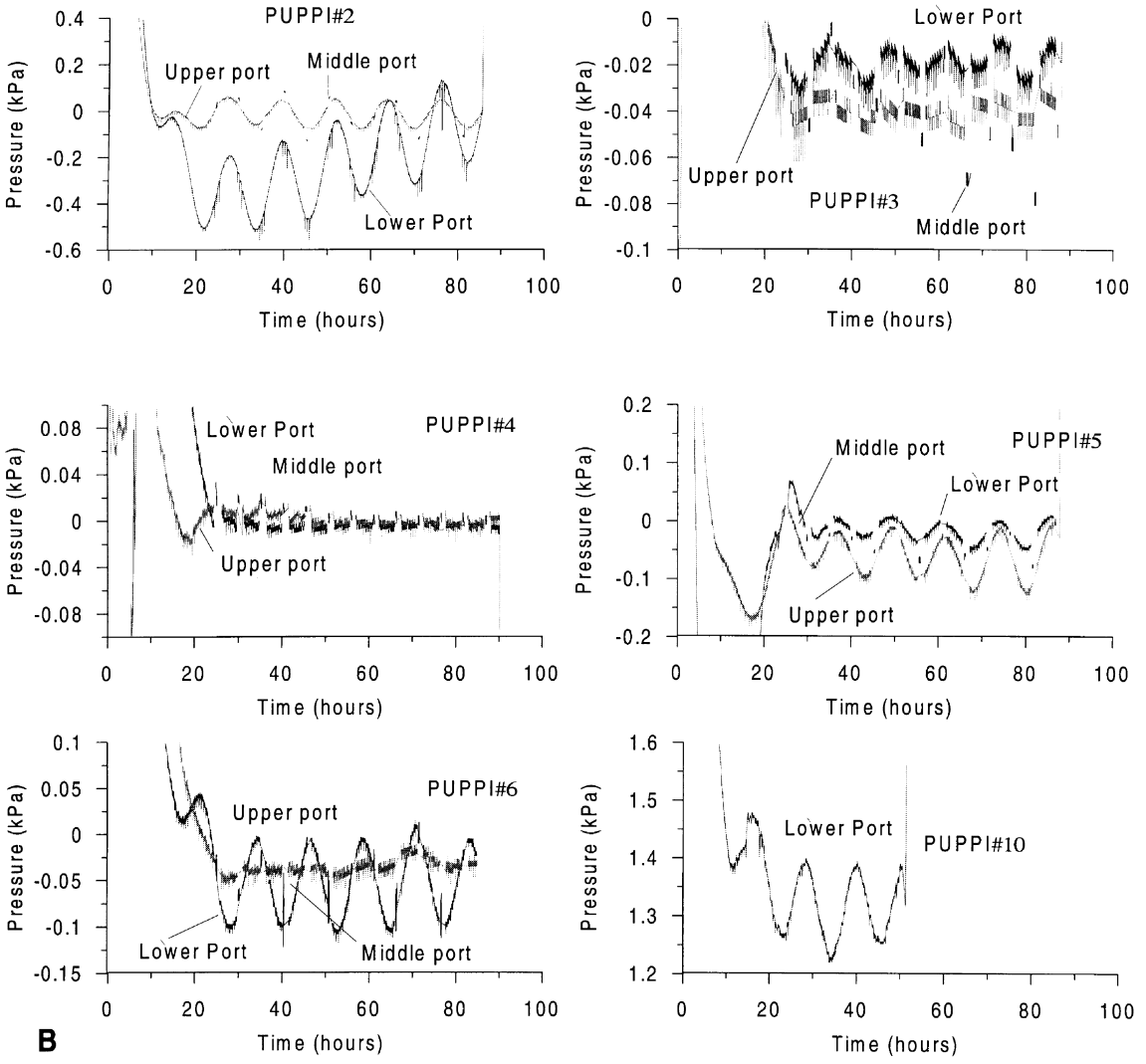

Fig. 3. (*continued*)

can be programmed to operate at any time during the measurement period. The valve closes and isolates the pressure ports on the lance whilst opening the differential pressure transducers to seawater. In this way reference zero pressures can be obtained at any time during the deployment and hence any drift monitored by regular zero measurements. Likewise, the valve can be used to enable a single pressure transducer to monitor more than one pressure port. Accordingly, one of the two transducers was set to sporadically monitor the third middle port.

Just prior to recovery an acoustic command is normally sent to the instrument to activate the pre-release pipe cutter. This opens both sides of each differential pressure transducer to the open seawater, hence providing an in situ zero pressure calibration just before recovery. Recovery is accomplished using an acoustic command, which activates a release mechanism severing the disposable from recoverable parts; the lance and ballast weight assembly is left on the seafloor while the buoyant instrument package ascends to the surface for recovery (Fig. 2). In addition to the acoustic command for release, the instrument

also houses a back-up release timer that can be set to release the instrument at any required time.

3.2. Analysis of the data

In addition to the ambient pore pressure (u_e), the pore pressure transients produced by the penetration of the PUPPI probe and by tidally induced pressure variations on the seafloor also provide information of hydrogeological and geotechnical interest. The maximum insertion pressure (u_{max}) is indicative of the shear strength (S_u) whilst modelling of the decay curve and tidally induced signals can provide estimates of the permeability (K) and confined frame compressibility (m_v) of the sediments (Schultheiss, 1990b; Fang et al., 1993; Wang and Davis, 1996; Wang et al., 1998).

At low penetration rates a spherical pore pressure distribution develops in the vicinity of the tip, whereas along the shaft the distribution tends to be more radial. At higher penetration rates this spherical distribution around the tip becomes more oblate or radial in nature and similar to that generated along the shaft (Elsworth, 1991). Therefore, estimates of the value of K can be obtained by modelling in two dimensions the expansion of a cylindrical cavity for undrained distributions of pore pressures at both, the upper and lower ports. Bennett et al. (1982) used the solutions of Soderberg (1962) and Randolph et al. (1979) to predict the permeability from the time taken for 50% of u_{max} to dissipate (t_{50}):

$$K = \mu m_v r_0^2 \tau_{50}/t_{50} \quad (1)$$

in which μ is the viscosity of seawater (1.656×10^{-3} Pa s), m_v the sediment confined frame compressibility as obtained from Eq. (2) (see below), r_0 the radius of the probe, t_{50} the time for pore pressure to fall to 50% of its initial value, and τ_{50} is the t_{50} related dimensionless time factor. Several studies (Bennett et al., 1982; Schultheiss and Noel, 1987; Schultheiss, 1990b; Davis et al., 1991) assumed the value of τ_{50} to be unity based, but more recently Fang et al. (1993) indicated that this could cause the value of K to be in error by one order of magnitude. Fang (1995) shows that more suitable values for τ_{50} are 3.93 at the ports on the probe shaft and 4.65 at the lower port. The middle port is only monitored seldom and can not provide values of t_{50}. It is to be noted that this analysis provides property estimates in the horizontal dimension, while physical properties measured in the laboratory are generally derived from vertical samples. However, in clay-rich sediments anisotropic conditions may exist. In sediments with a random soil fabric (as might be expected for deep marine mud) nearly isotropic conditions generally exist (Bennett et al., 1982). This must be accounted for when expressions involve both types of parameters. Eq. (1) also assumes that insertion of the probe does not change the permeability of the sediment, and that the sediment–probe interface does not act as a channel with permeability higher than that of the sediments (Fang, 1995).

In addition, to the insertion pressure, small oscillations of the pore pressure induced by ocean tides can be observed on the PUPPI records (Fig. 3). Ocean tides generate oscillations of water pressure at the sea bottom. Deformation of the sediment as well as fluid flow is simultaneously induced in response to the tidal pressure variations since the sediment behaves as a porous medium. Fang et al. (1993) gave simplified formulae allowing to estimate the confined frame compressibility (m_v) from the amplitude of the tidally induced pore pressure variations (u_t). The formulae modified according to Wang and Davis (1996) is:

$$u_t \cong Q \frac{n\beta_f}{n\beta_f + m_v} \quad (2)$$

where Q is the amplitude of the seafloor pressure variation (6.5 kPa), n the fractional porosity as determined by Roberts and Cramp (1996) (0.7) and β_f the compressibility of the pore fluid, seawater (4.54×10^{-10} Pa^{-1}).

Direct in situ measurements of pore pressure gradients in seafloor sediments is also one of the primary ways to detect and quantify fluid flow through the seafloor and to estimate the sub-seafloor pressures at greater depths. The rates of pore fluid flow are related to the pore pressure gradient through Darcy's law, i.e. the flux of pore fluid is proportional to the pore pressure gradient times the permeability. Thus the seepage velocity (v) of an element of water in the soil can be expressed as:

$$v = K u_e/\mu z n \quad (3)$$

where z is the depth of the port measuring the pore pressure.

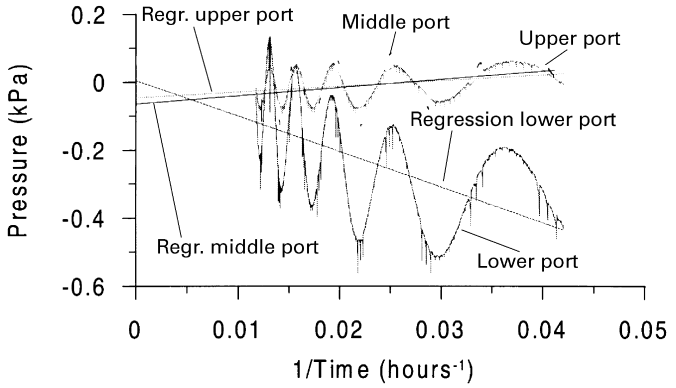

Fig. 4. Extrapolation of the last hours of the pore pressure decay vs. the reciprocal of time for PUPPI #2. At 1/time = 0 (i.e. time = ∞) the pore pressure is assumed to be the ambient or equilibrium pore pressure.

The pore pressure data was also used in combination with sediment core data from Roberts and Cramp (1996) to assess the effect of non-hydrostatic pore pressures on sediment stability under cyclic loading. To this purpose we re-examined the results of Roberts and Cramp (1996) with the newly obtained pore pressure measurements. In their study, they estimate a horizontal ground acceleration expressed as a fraction of gravity, k, from the normalised strength parameter (S) and the maximum past stress (σ'_{vm}) (Lee and Edwards, 1986):

$$k = \frac{\gamma'}{\gamma}\left[A_c A_r U S \left(\frac{\sigma'_{vm}}{\sigma'_v}\right)^m - \sin\alpha\right] \quad (4)$$

where A_c is the correction for anisotropic consolidation, A_r the correction for cyclic loading, m the sediment parameter typically about 0.8, γ' the effective sediment unit weight, γ the total wet sediment unit weight, σ'_v the overburden pressure, which in turn can be expressed as a function of depth in sediment ($\sigma'_v = \gamma' z - u_e$), and U the ratio σ'_v to $\gamma' z$. The ratio σ'_{vm}/σ'_v is also designated as the overconsolidation ratio (OCR).

4. Results

4.1. Ambient pore pressures

At the end of the recording period at all PUPPI deployments, pore pressures were close to equilibrium but still slightly descending. To avoid the influence of the high initial insertion pressures, we estimated the equilibrium pressure by plotting the pressure record from 25 h after penetration until recovery vs. the reciprocal of time and extrapolating to 1/time = 0 (Fig. 4), a technique suggested by Davis et al. (1991) and Fang et al. (1993).

The ambient pore pressures estimated for the lower ports of all deployments are usually higher than those estimated for the middle and upper ports (except for PUPPI #6) (Fig. 5). The lower port of the westernmost deployment (#10), at the edge of the Canary Debris Flow, shows the only evidences of substantial excess pore pressures which reach 1322 Pa. This suggests that excess pore pressures might have played an important role in the past in triggering the Canary Debris Flow (see further discussion).

In general all the deployments show that the ambient pore pressures within the first 4 m of the sediment column are negative (Table 2). This is always the case for ambient pore pressures in the upper and middle ports, with values ranging from 0 Pa at the lower port of deployment 2 to −72 Pa recorded at the middle port of deployment 3. The deployments do not show a single trend of pore water pressure increase or decrease which could be interpreted as a downward constant pressure gradient. In general the middle ports show more negative values (from −11 to −72 Pa) than those at the upper (from −9 to −85 Pa) and lower ports (1322 to −46 Pa). The exception is deployment number 5, with an upper value of −85 Pa and a middle value of −64 Pa (Fig. 5). This is clearly shown by the total and between ports

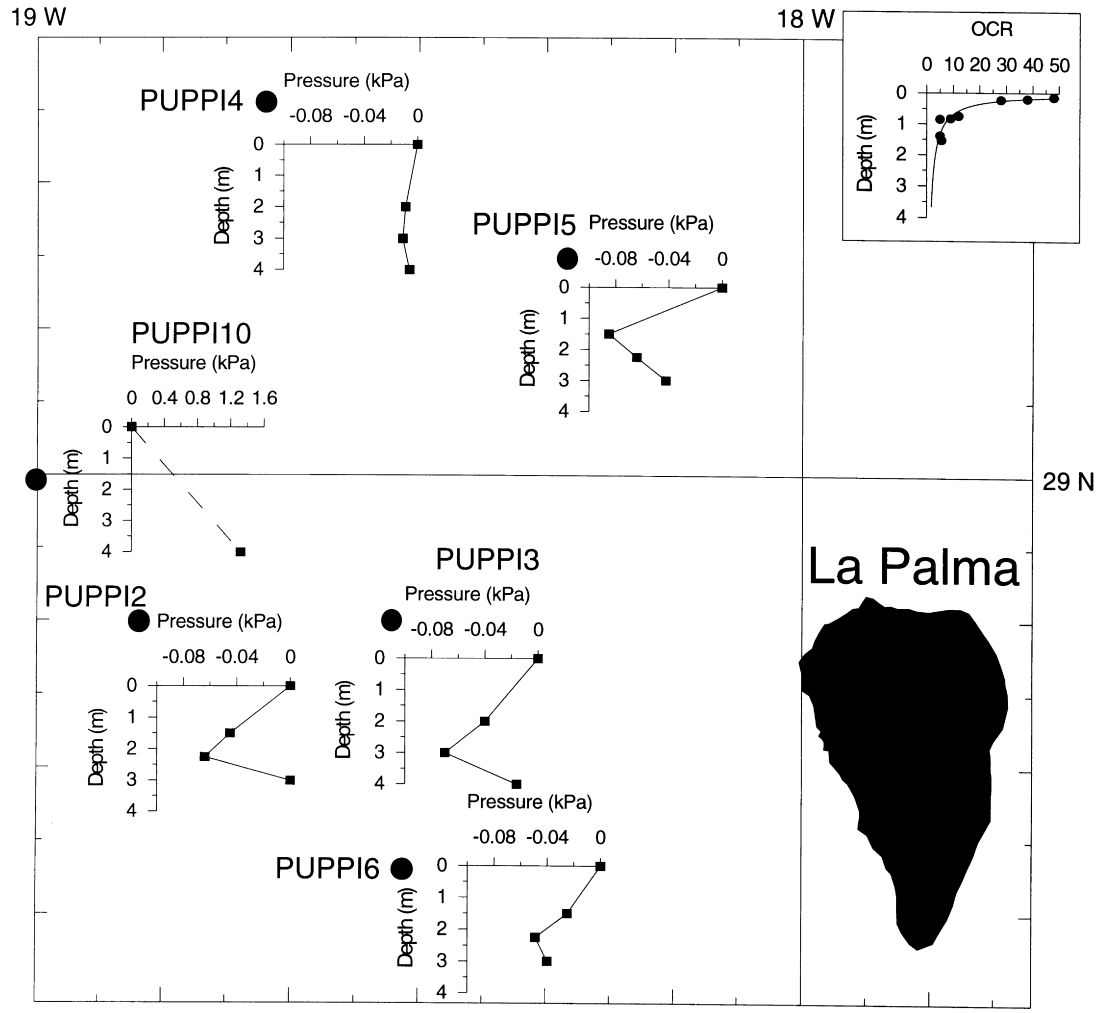

Fig. 5. Excess pore pressure (kPa) vs. depth in *y*-axis (m) located geographically. PUPPI #10 is shown with a dashed line since only the record of the lower port is available. Note that the *x*-axis is not drawn at the same scale in all the deployments. An exponential fit plot of OCR vs. depth as depicted from the data (circles) of Roberts and Cramp (1996) is also shown on the top right-hand corner. This shows the maximum depth to which the equilibrium pressure estimates might be influenced by overconsolidation.

pressure gradients in Table 2. In most of the cases, the total pressure gradients are negative but, in contrast, the pressure gradient between the middle and lower ports is always positive.

The distribution of pore pressures can be explained by the model of Fig. 6 in which the negative pore pressures appear closer to the island of La Palma and the positive pore pressures off the island flanks. It can also be observed that the negative pore pressures display, in overall, a wedge thickening towards the island of La Palma (Fig. 6).

4.2. Maximum insertion pressures and half decay times

The maximum insertion pressures of the sediments recorded by the probes are highly variable. This is an important point since they are directly related to the shear strength of the sediment. The maximum insertion pressures range from 81611 Pa recorded at the lower port of PUPPI #2 to 340 Pa recorded at the upper port of PUPPI #4. In fact, at some sites the insertion pressures were very small (Table 2)(PUPPI 3

Table 2
PUPPI recorded data summary

Station number		Depth of port (m)	Equilibrium pressure (kPa)	Maximum insertion pressure (kPa)	t_{50} (s)	Pressure gradient (kPa m^{-1})		Tidal cycle amplitude (kPa)
						Total	Between ports	
PUPPI 2	Upper port	1.5	−0.045	35.917	355.32	−0.030		0.12
	Middle port	2.25	−0.064			−0.028	−0.025	0.207
	Lower port	3	≈ 0	81.611	31.32	0	0.085	0.32
PUPPI 3	Upper port	2	−0.040	0.463	101.16	−0.020		0.014
	Middle port	3	−0.072			−0.024	−0.032	0.038
	Lower port	4	−0.016	10.317	4.295	−0.004	0.056	0.029
PUPPI 4	Upper port	2	−0.009	0.341	658.8	−0.004		
	Middle port	3	−0.011			−0.004	−0.002	
	Lower port	4	−0.006	0.447	18	−0.001	0.005	
PUPPI 5	Upper port	1.5	−0.085	80.369	352.8	−0.056		0.071
	Middle port	2.25	−0.064			−0.028	0.028	0.046
	Lower port	3	−0.042	23.334	34.92	−0.014	0.029	0.038
PUPPI 6	Upper port	1.5	−0.025	1.053	17734.68	−0.016		0.015
	Middle port	2.25	−0.049			−0.021	−0.032	0.077
	Lower port	3	−0.040	19.146	10.2	−0.013	0.012	0.090
PUPPI 10	Upper port	2		46.703	175.32			
	Lower port	4	1.322	41.962	571.32	0.331		0.152

upper port, PUPPI #4 and PUPPI #6 upper port). There are three possible reasons for this: (1) the decay rate is too great for the sampling rate (6 s), and thus the maximum insertion pressure was not recorded; (2) there was little or no penetration; or (3) the sediments have a very low shear strength.

Where low insertion pressures were recorded t_{50} shows generally low values and tidal cycles have low amplitudes or are not present in the record. These two factors suggest that the sediments have high permeability (i.e. the peak insertion pressures were not recorded) and low shear strengths (see Table 3). An exception to this is PUPPI site #6 where the upper port recorded a low insertion pressure but t_{50} is 17734 s, probably anomalous due to an unsampled higher insertion pressure (note the t_{50} at the lower port of 10.2 s).

4.3. Estimated compressibility and permeability

In comparison with the core data reported by Roberts and Cramp (1996) the permeability estimates derived from the pore pressure data are generally one order of magnitude lower. Estimates of permeability from dissipation data (Eq. (1)) are highly variable and range between 2.5×10^{-18} to 6.6×10^{-16} m^2. The average estimated permeabilities from each site show a graded distribution from proximal to distal consequent with their relative location to the detrital source areas. The confined frame compressibilities (Eq. (2)) range between 6.2×10^{-9} and 1.5×10^{-7} Pa^{-1} and, in the same manner than permeability, are about one order of magnitude less than the mean determined from core data (Roberts and Cramp, 1996). Compressibilities and, in turn, permeabilities can be underestimated since we are using the confined frame compressibility derived from the unloading/reloading curves, while in consolidation models it generally used the compressibility derived from the virgin loading curve (Fang et al., 1993).

Table 3 shows that, at most sites, the permeability is lower for the upper port than for the lower port, while compressibility is higher at the upper port than at the lower port. This suggests that the sediments might be

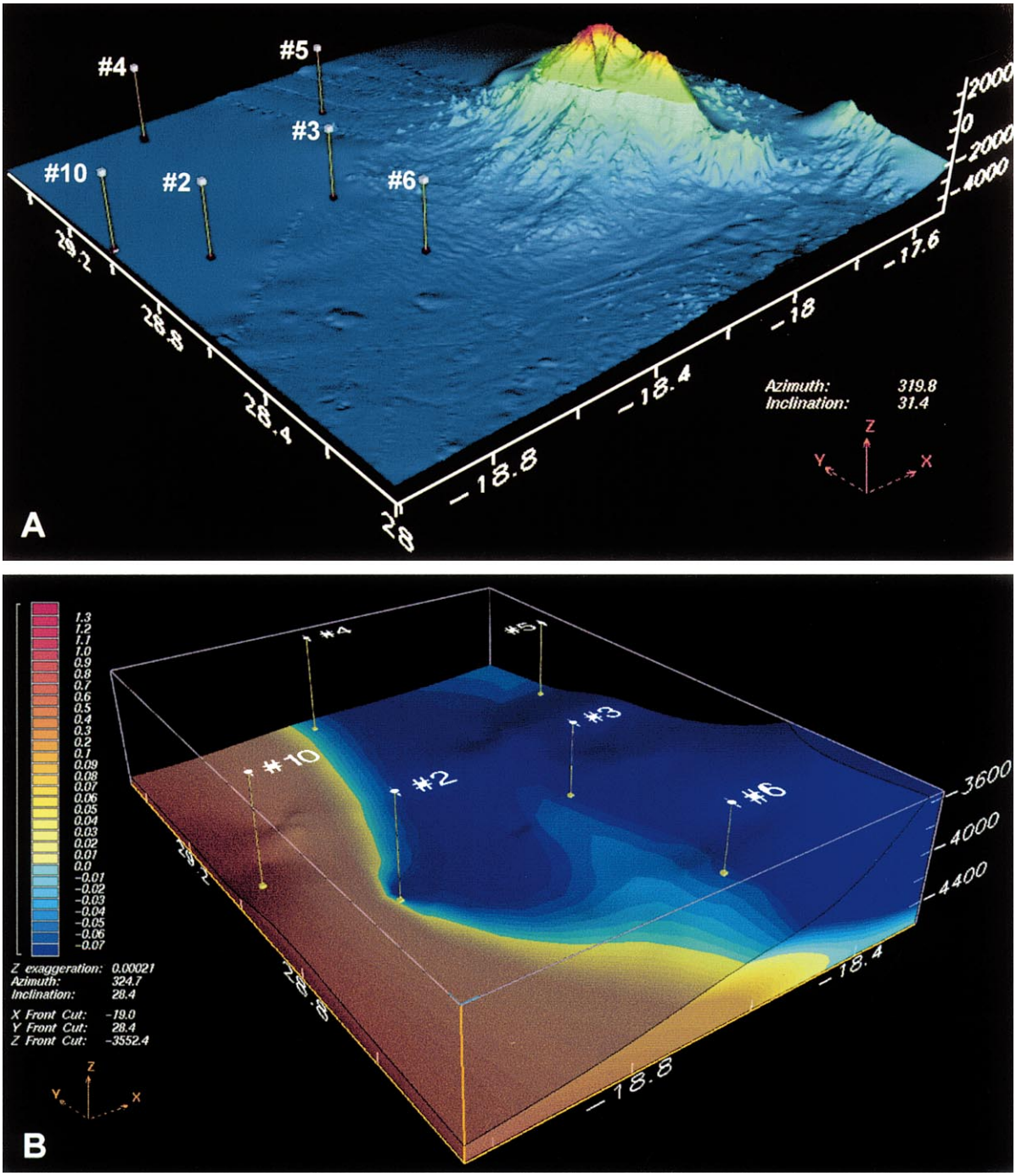

Fig. 6. Perspective view of the Island of La Palma from swath bathymetry and digitised on land contours (data from Urgeles et al., 1999) with location of the PUPPI sites (A); and 3D model view showing the bathymetry of the area surveyed with the PUPPIs and the distribution of pore pressures within the first 5 m of sediment (B). Vertical scale is magnified 50 times and the interval with pore pressure records is magnified 20 times with respect to the topographic scale.

Table 3
Estimated permeability, confined frame compressibility, seepage velocity and shear strength

Station number		Compressibility (m_v) $\times 10^{-8}$ (Pa^{-1})	Permeability[a] (K) $\times 10^{-17}$ (m^2)	Seepage velocity[b] (v) (mm y^{-1})	Shear strength[c] (S_u) (kPa)
PUPPI 2	Upper	3.54	2.70	−0.0221	13.60
	Lower	0.62	3.57	0	5.98
PUPPI 3	Upper	14.95	66.54	−0.3620	0.07
	Lower	7.20	1.01	−0.0011	1.71
PUPPI 4	Upper	–	2.54	−0.0031	0.05
	Lower	–	5.47	−0.0022	0.07
PUPPI 5	Upper	2.92	4.90	−0.0755	13.39
	Lower	5.49	17.85	−0.0679	3.88
PUPPI6	Upper	13.95	0.25	−0.0011	0.17
	Lower	2.29	39.32	−0.1426	3.19
PUPPI 10	Upper	–	1.83	–	7.78
	Lower	1.35	1.65	0.1487	6.99

[a] Permeabilities at sites where tidal oscillations are not observed were estimated from the mean m_v.
[b] Seepage velocities are calculated with respect to the total pressure gradient.
[c] Inferred from the empirical relation $S_u = u_{imax}/6$.

overconsolidated in the first two metres of the sediment column. This is in agreement with data from Roberts and Cramp (1996) which show that the first meter of sediment is overconsolidated (see also Fig. 5). It is known from several studies that the typical overcompaction of deep-sea sediments may be due to various causes including erosion, ageing, initial cementation, sediment reworking and bioturbation. Induced tidal pressure oscillations, which are observed in almost all deployments, is the most likely cause of sediment overcompaction.

4.4. Slope stability analysis

The slope stability analysis was performed according to the method of Lee and Edwards (1986) (see Eq. (4)), that assess the stability of a slope undergoing seismic load. The values for the sediment density (γ), friction angle (Φ), normalised strength parameter (S) and past overburden pressure (σ'_{vm}) were obtained from Roberts and Cramp (1996). Two of the selected PUPPI sites (#3 and #10) correspond to core sites from Roberts and Cramp (1996) (Fig. 1), and thus, the results here presented can be directly compared to the geotechnical measurements made on these cores.

It is also to be noted that the excess pore pressures are mainly negative (Table 2 or Table 4) and, thus, this parameter will reinforce sediment stability instead of favouring failure. Only PUPPI #10, located at the edge of the Canary Debris Flow, shows positive excess pore pressures in such amount that would be able to reduce significantly (6%) the value of k.

We observe that the method of Lee and Edwards (1986) is also quite influenced by the OCR. If we assume that the values of OCR are actual and present at depth, the values of k range between 0.832 and 0.2. If the overconsolidation is apparent and the sediments are normally consolidated (OCR = 1), as deduced west of La Palma by Roberts and Cramp (1996) and other settings (Baraza et al., 1990), then the values of k range between 0.187 and 0.133. The effects of excess pore pressure are much more significant when the sediments are normally consolidated inducing variations in the value of k in excess of 6%.

5. Discussion

5.1. Fluid flow and seepage velocities

From our data, it is evident that the ambient pore

Table 4
Reassessment of the slope stability

Core number	Depth (m)	Pressure gradient (Pa m^{-1})	Estimated excess pore pressure (Pa)	γ_{sw} (N m^{-3})	γ (N m^{-3})	α (°)	S	Induced OCR	k	k if $u_e = 0$	(%)[a]
CD56-24	0.14	330.5 (PUPPI #10)	46.27				0.74	1	0.187	0.199	
	0.83		274.31		15535	0.25	0.53	1	0.133	0.142	6.3
	1.39		459.39	10253			0.57	1	0.143	0.153	
CD56-26	0.23	−20 (PUPPI #3)	−4.60		15774	0.8	0.66	1	0.180	0.179	
	0.85		−17.00				0.54	1	0.146	0.146	−0.37

[a] Negative percentages indicate increase in the value of k.

pressures found on the sediments on the western flank of La Palma are not the typical one should expect on a passive margin (i.e. mainly excess pore pressures generated by fluid expulsion due to sediment compaction). In this setting, it would have been reasonable to expect that sediment loading by volcanic material produced by ocean island growth would contribute to enhance this effect. There is not, however, a clear trend on the pore pressure profiles on Fig. 5. Although all of the measurements show negative pore pressures at all ports with the given exception of the westernmost deployment, the gradients between ports clearly show that there is not a simple constant pressure gradient with depth (Table 2). Likewise, it is known that an increase in shear stress, such as the probe penetration, may induce a dilatancy in overconsolidated clays (Imai and Xie, 1990). This is usually accompanied by the generation of transient negative pore pressures such as those of PUPPI #5 (Fig. 3B) but the length of the measurement period as well as the extrapolation to time $= \infty$ should neutralise this effect. In addition, the data of Roberts and Cramp (1996) indicate that overconsolidation does not extend deeper than 2 m while the lower ports recording negative pressures are 4 m below the sea floor (Fig. 5).

A possible explanation for the opposed between ports gradient is that lateral advection occurs taking advantage of more permeable media such as volcanoclastic turbidite sands. It is normally assumed that in deep marine conditions fluid flow would occur vertically in the lowly permeable sediment section and laterally through the highly permeable oceanic basement. Nevertheless, the turbidite layers that are interbedded with the hemipelagic sediments may act as minor inflow layers (compared to the oceanic basement).

Although flow regimes might be quite different, analogies can be found in continental sedimentary basins. In these settings, cross flow might be present which may even lead to opposite fluid flow regimes in low permeability formations (Alexander et al., 1987). A revision of the literature where data from pore pressure probes was analysed (Hirst and Richards, 1976; Bennett et al., 1982; Davis et al., 1986, 1991; Schultheiss and Noel, 1987; Langseth et al., 1992; Fang et al., 1993; Bennett et al., 1996; Harvey et al., 1998) shows that only one or two pressure ports where used in estimating pore fluid pressures. The data from those probes will always provide a single pressure gradient trend. However, using several ports would have probably shown a more complex pattern of fluid circulation in which different permeability layers also influence the fluid circulation.

As a general rule, we observe that the fluid flow occurs downward (Table 3). The exception is PUPPI #10, which is the distal most deployment. Conceiving the causes of such a distribution of pore pressures is not easy if thermal effects associated to the volcanic activity in the island of La Palma are not taken into account. We think that the “anomalous” results observed off La Palma could be due to the effect of a hot spot-related hydrothermal cell superimposed to the typical expulsion of fluids on a passive margin (Fig. 7). This is consequent with the data presented on the 3D model of Fig. 6, where a wedge of negative pore pressures, indicating downward fluid flow,

thickens towards La Palma. Such a hydrothermal cell would extend for about 100 km, that can be compared to those of other hot spots such as the Marquesas or the Hawaiian ones, with cells extending 150 and 25 km, respectively (Garven and McNutt, 1995). It remains unclear, however, whether the hydrothermal cell is associated with the volcanism on the La Palma edifice alone or to a broader thermal anomaly related to the hot spot. It is also important to remark that evidence of hydrothermal activity has been found offshore mid-plate ocean islands, where hydrothermal vents are also present (Malahoff et al., 1982; Cheminée et al., 1991). The excess pore pressures, typical of a passive margin, are then found to be away from the island flanks as shown in Fig. 7, but positive pore pressures are also expected in the more proximal areas driven by the thermal anomalies.

Estimates of the flow seepage velocities (v) were obtained following Darcy's law (Eq. (3)). Permeabilities from insertion pressure dissipation times indicate that the downward seepage velocities range between -0.001 and -0.3 mm y^{-1}, respectively. These numbers would imply greater fluid flow than those found from PUPPI results in the Madeira Abyssal Plain, which shows almost no flow (Schultheiss and Noel, 1987). On the other hand, the rates of fluid flow are lower than those encountered in the sediment fields near mid-ocean ridges with downward velocities ranging between -2 and -7 mm y^{-1} (Fang et al., 1993) and upward velocities of 15 mm y^{-1} (Davis et al., 1991). Although the calculated flow velocities can be considered very low, a strong thermal anomaly must be present to induce hydrothermal circulation in sediments exceeding 1 km in thickness.

At the westernmost PUPPI #10 the measured upward fluid flow can not be maintained alone by typical sedimentation rates in the study area, currently averaging 60 m Ma^{-1}. However, when loading by the adjacent islands of El Hierro and La Palma is considered, then the upward fluid flow can be easily accounted for.

5.2. Implications of a hot spot-related hydrothermal cell

The intersection of a hydrothermal cell with the seafloor surface implies both a zone where fluids flow downwards and a zone, usually more concentrated (e.g. hydrothermal vents), where fluid flows upwards. Since, within the hypothetical hydrothermal cell, the data presented in this study only show evidence for downward fluid flow, we presume that upward flow should occur somewhere in the more proximal island flanks. It is known that very characteristic hydrothermal vents, in terms of compositional and thermal differences, may occur in ocean islands (Malahoff et al., 1982) but very few observations have been done in islands other than Hawaii. Thus, the submarine ridges around La Palma, an island where the last subaerial eruption occurred in 1971 (Carracedo, 1994), could be one of the primary targets worldwide, for searching for such hydrothermal vents.

It is also worth remarking that the upward fluid flow that might be occurring in the more proximal island flanks will reduce the shear strength of the volcanic materials and therefore could be one of the primary factors enhancing the trigger of giant volcanic landslides and debris avalanches. Again, La Palma is a good example for that, since the fissures that opened during the 1949 eruption on the southern Cumbre Nueva Ridge (Bonelli Rubio, 1950) are believed to correspond to the initial stage of one of these giant landslides (Carracedo, 1994).

5.3. The role of pore pressure in triggering sediment landslides

It is known that the region surveyed with the PUPPIs has undergone large sediment failures such as the Canary Debris Flow, involving volumes of up to 400 km^3 (Masson et al., 1992). However, from the slope stability results it is clear that the sediment wave field west of the island of La Palma is at present a stable feature. For that reason we need to invoke external factors to generate such increments of pore pressure that allow the triggering of these huge debris flows. Roberts and Cramp (1996) propose that the Canary Debris Flow could have been triggered by loading of the slope by the El Golfo Debris Avalanche, a deposit related to the lateral collapse of the northern flank of the edifice of El Hierro.

It is also important to admit that the pore pressure may have not remained constant over time. There have been important reorganisations of the volcanism within the rift system in La Palma (Carracedo et al., 1997), which might have altered hydrothermal

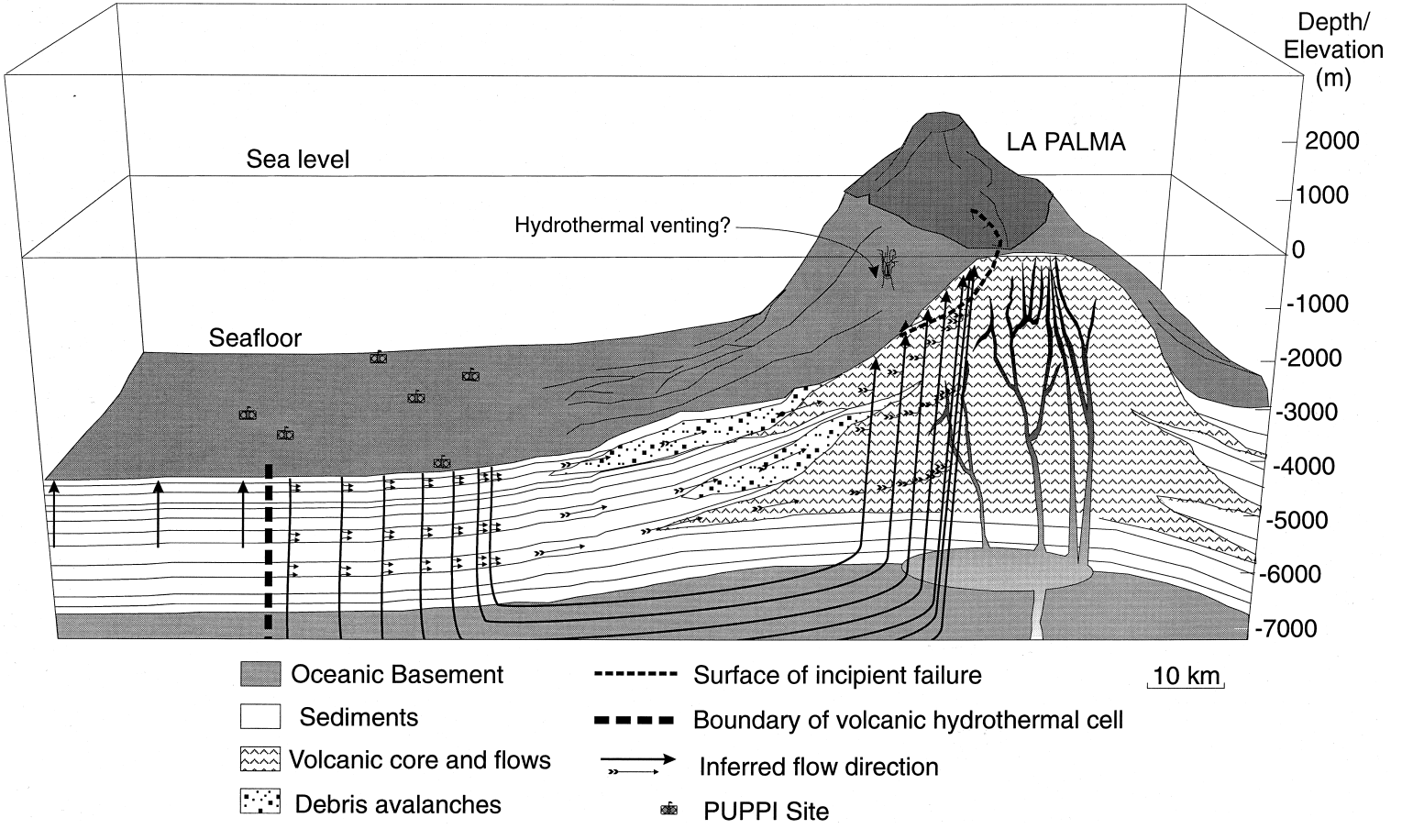

Fig. 7. Model of fluid flow path on the flanks of an oceanic island as shown by the distribution of ambient pore pressures recorded by the PUPPI apparatus. Depth of shallow magma chambers as inferred from Kluegel et al. (1997), with uplifted basement inferred from Urgeles et al. (1998).

circulation. For example, since about 7 ka, the distribution of volcanic vents in the southern rift has changed completely and activity has concentrated along the north–south rift, which has extended northwards (Carracedo et al., 1997). Such reorganisations may consequently induce radical changes of the associated hydrothermal cell ranging from a simple redistribution to the complete disappearance of the cell in periods of magmatic quiescence. For that reason, in some periods the pore pressures could have been much higher than nowadays, being more favourable to trigger landslides in the sedimentary piles adjacent to the volcanic flanks. This implies that in this area the thermal diffusivity is larger than the hydraulic diffusivity, which is plausible given the permeabilities of the sedimentary materials, the overall sediment thickness and the extent of the hydrothermal cell.

5.4. Further developments and studies

Along with this study we have presented a pore pressure model (Fig. 6) that fits the data observed in six probes. The model is simplistic since the data, which are costly to obtain, are scarce. Thus, the development of longer pore pressure probes able to achieve more rapidly the dissipation of the excess pore pressures would enhance the possibility for a greater number of deployments while giving data from deeper horizons. This would also allow dissipating some doubts concerning the nature of the negative pore pressures in relation to sediment consolidation risen in this article.

Pursuing the study of fluid flow and effects of pore pressure on the stability of island flanks requires the deployment of more probes around oceanic islands. Heat flow measurements may also help us to understand fluid circulation in this context as well as the role of such process in creating excess pore pressures. Future studies should include the use of instrumented sleds and submersibles searching for hydrothermal vents, with the aim to increase understanding of the thermal and hydrologic regimes in and around hot spot-related oceanic islands.

6. Conclusions

The PUPPI instrument has proven to be of great value for obtaining in situ high-quality pore pressure data and permeabilities, as well as to assess fluid flow and sediment stability. The ambient pore pressures recorded off west La Palma are negative in most of the cases, generally on the order of 0 to -85 Pa. Excess pore pressures are only present in the most distal areas.

The compressibilities estimated from the amplitude of the pore pressure variation induced by tides range between 6.2×10^{-9} and 1.5×10^{-7} Pa^{-1}. The permeabilities estimated from the dissipation data and the above compressibilities range between 2.5×10^{-18} and 6.6×10^{-16} m^2. The estimated permeabilities are usually higher for the lower port suggesting that the first 2 m of sediment might be overconsolidated.

Reassessment of the stability according to the data in Roberts and Cramp (1996) and to the PUPPI data presented in this paper shows that the sediment field on the western flank of La Palma is a stable feature. Induced accelerations on the seafloor of the range 0.187–0.133 g (if normal consolidation of the sediments is assumed) are needed to trigger new sediment landslides. The ambient pore pressures encountered in the study area have shown to favour stability and only deployment #10 shows excess pore pressures in such amount to be able to reduce the critical acceleration factor by 6%.

The data presented in this paper show that fluid flow recorded by the PUPPIs is, in most of the cases, abnormal for a classical passive margin where we would expect an upwards flow instead of downwards. This is interpreted as the superposition to the release of pore fluids by compaction on the continental rise, of a 100 km wide hydrothermal cell, related to the volcanic activity on the island of La Palma.

Estimates of seepage velocity range between 0 and -0.3 mm y^{-1} for the downward fluid flow related to the hydrothermal cell, and of 0.14 mm y^{-1} for estimates of fluid flow outside the area of thermal influence.

The occurrence of such convective cell related to the volcanic activity could generate excess pore pressures on the proximal flanks of the island that would significantly enhance the triggering of giant volcanic landslides.

7. Data accessibility

Pore pressure data recorded by all deployments

is accessible upon request to Miquel Canals (miquel@natura.geo.ub.es).

Acknowledgements

This work has been supported by the projects MAR98-0347 (GRANDES) and AMB94-0323 (CRESCENT), funded by the Spanish National Agency for Science and Technology (CICYT), the European Union MAST-II Programme, project number MAS2-CT94-0083 (STEAM), and the "Comissionat per a Universitats i Recerca" (C.U.R.) of the "Generalitat de Catalunya", project 1997SGR-80. R. Urgeles held a Fellowship of the C.U.R. We particularly thank Derek Elsworth, Kelin Wang, Marcel Hürlimann and Mark Randolph for their help while writing this manuscript. Critical reviews by D. Abbott, P. Cochonat, E.E. Davis, R.P. von Herzen and an anonymous reviewer are also acknowledged. Special thanks are given to Julio Robert, master of the SNV *Las Palmas* whose enthusiasm and dedication allowed the campaign to take place. Thanks are also due to the master of the RRS *Discovery* and crews of the two vessels for their efficiency and co-operation.

References

Alexander, J., Black, J.H., Brightman, M.A., 1987. The role of low-permeability rocks in regional flow. In: Goff, J.C., Williams, B.P.J. (Eds.), Fluid Flow in Sedimentary Basins and Aquifers. Geological Society Special Publication 34, 173–183.

Ancochea, E., Hernán, E., Cendrero, A., Cantagrel, J.M., Fúster, J.M., Ibarrola, E., Coello, J., 1994. Constructive and destructive episodes in the building of a young oceanic island La Palma, Canary Islands, and the genesis of the Caldera de Taburiente. Journal of Volcanology and Geothermal Research 60, 243–262.

Baligh, M.M., 1986. Undrained deep penetration II, Pore pressures. Géotechnique 36, 487–501.

Baraza, J., Lee, J.L., Kayen, R.E., Hampton, M.A., 1990. Geotechnical characteristics and slope stability on the Ebro margin, western Mediterranean. Marine Geology 95, 379–393.

Bea, R.G., Bernard, H.A., Arnold, P., Doyle, E.H., 1975. Soil movements and forces developed by wave-induced slides in the Mississippi Delta. Journal of Petroleum Technology 27, 500–514.

Bennett, R.H., Burns, J.T., Clarke, T.L., Faris, J.R., Forde, E.B., Richards, A.F., 1982. Piezometer probes for assessing effective stress and stability in submarine sediments. In: Saxov, S., Nieuwenhuis, J.K. (Eds.), Marine Slides and other Mass Movements. Plenum, New York, pp. 129–161.

Bennett, R.H., Hulbert, M.H., Meyer, M.M., Lavoie, D.M., Briggs, K.B., Lavoie, D.L., Baerwald, R.J., Chiou, W.A., 1996. Fundamental response of pore-water pressure to microfabric and permeability characteristics: Eckernförde Bay. Geo-Marine Letters 16, 182–188.

Bonelli Rubio, J.M., 1950. Contribución al estudio de la erupción del Nambroque o San Juan (Isla de la Palma), Instituto Geográfico y Catastral, Madrid, Spain.

Carracedo, J.C., 1994. The Canary Islands: an example of structural control on the growth of large oceanic-islands volcanoes. Journal of Volcanology and Geothermal Research 60, 225–241.

Carracedo, J.C., Day, S.J., Guillou, H., 1997. Late (Quaternary) shield-stage volcanism in La Palma and El Hierro, Canary Islands, International workshop on volcanism and volcanic hazards in immature intraplate oceanic islands. Estación Volcanológica de Canarias, La Palma, Canary Islands, Spain, pp. 59–66.

Cheminée, J.-L., Stoffers, P., McMurtry, G., Richnow, H., Puteanus, D., Sedwick, P., 1991. Gas-rich submarine exhalations during the eruption of Macdonald Seamount. Earth Planetary Science Letters 107, 318–327.

Davis, E.E., Goodfellow, W.D., Bornhold, B.D., Adshead, J., Blaise, H., Villinger, H., Le Cheminant, G.M., 1986. Massive sulfides in a sedimented rift valley, northern Juan de Fuca Ridge. Earth and Planetary Science Letters 82, 49–61.

Davis, E.E., Horel, G.C., MacDonald, R.D., 1991. Pore pressures and permeabilities measured in marine sediments with a tethered probe. Journal of Geophysical Research 96, 5975–5984.

Elsworth, D., 1991. Dislocation analysis of penetration in saturated porous media. Journal of Engineering Mechanics 117, 391–408.

Fang, W.W., 1995. Fluid flow in upper oceanic crust: In situ measurement and numerical modelling. PhD thesis, Columbia University, New York, USA.

Fang, W.W., Langseth, M.G., Schultheiss, P.J., 1993. Analysis and application of in situ pore pressure measurements in marine sediments. Journal of Geophysical Research 98, 7921–7938.

Garven, G., McNutt, M.K., 1995. Hydrogeologic modeling of archipelagic aprons. Geological Society of America Abstracts with Programs 27, 429.

Harvey, F.E., Rudolph, D.L., Frape, S.K., 1998. Measurement of hydraulic properties in deep lake sediments using a tethered pore pressure probe: applications in the Hamilton Harbour, western Lake Ontario. Water Resources Research 33, 1917–1928.

Hirst, T.J., Richards, A.F., 1976. Excess pore pressure in Mississipi Delta sediments: initial report. Marine Geotechnology 1, 337–344.

Hoernle, K.A., Schmincke, H.-U., 1993. The role of partial melting in the 15-Ma geochemical evolution of Gran Canaria: a blob model for the Canary Hot Spot. Journal of Petrology 34, 594–626.

Holcomb, R.T., Searle, R.C., 1991. Large landslides from oceanic volcanoes. Marine Geotechnology 10, 19–32.

Imai, G., Xie, C., 1990. An endochronic constitutive law for static shear behaviour of overconsolidated clays. Soils and Foundations 30, 65–75.

Kidd, R.B., Simm, R.W., Searle, R.C., 1985. Sonar acoustic facies and sediment distribution on an area of deep ocean floor. Marine Petroleum Geology 2, 210–221.

Kluegel, A., Hansteen, T.H., Schmincke, H.-U., 1997. Rates of magma ascent and depths of magma reservoir beneath La Palma, Canary Islands. In: International Workshop on Volcanism and Volcanic Hazards in Immature Intraplate Oceanic Islands. Estación Volcanológica de Canarias, La Palma, Canary Islands, Spain, pp. 29–30.

Langseth, M.G., Becker, K., von Herzen, R.P., Schultheiss, P.J., 1992. Heat and fluid flux through sediment on the western flank of the Mid-Atlantic Ridge: a hydrogeological study of North Pond. Geophysical Research Letters 19, 517–520.

Lee, H.J., Edwards, B.D., 1986. Regional method to assess offshore slope stability. Journal of Geotechnical Engineering 112, 489–509.

Malahoff, A., McMurtry, G.M., Wiltshire, J.C., Yeh, H.W., 1982. Geology and chemistry of hydrothermal deposits from active submarine volcano Loihi, Hawaii. Nature 298, 234–239.

Masson, D.G., 1996. Catastrophic collapse of the volcanic island of Hierro 15 ka ago. Geology 24, 231–234.

Masson, D.G., Hugget, Q.J., Weaver, P.P.E., Brunsden, D., Kidd, R.B., 1992. The Saharan and Canary debris flows offshore Northwest Africa. Landslide News 6, 9–12.

Masson, D.G., Canals, M., Alonso, B., Urgeles, R., Huhnerbach, V., 1998. The Canary Debris Flow: source area morphology and failure mechanisms. Sedimentology 45, 411–432.

Randolph, M.F., Carter, J.P., Wroth, C.P., 1979. Driven piles in clay—the effects of installation and subsqeuent consolidation. Géotechnique 29, 361–393.

Ranero, C.R., Torne, M., Banda, E., 1995. Gravity and multichannel seismic reflection constraints on the lithospheric structure of the Canary Swell. Marine Geophysical Researches 17, 519–534.

Roberts, J.A., Cramp, A., 1996. Sediment stability on the western flanks of the Canary Islands. Marine Geology 134, 13–30.

Schultheiss, P.J., 1990. In-situ pore-pressure for a detailed geotechnical assessment of marine sediments: state of the art. In: Demars, K.R., Chaney, R.C. (Eds.), Geotechnical Engineering of Ocean Waste Disposal (ASTM STP 1087). American Society for Testing and Materials, Philadelphia, PA, pp. 190–205.

Schultheiss, P.J., 1990. Pore pressures in marine sediments: an overview of measurement techniques and some geological and engineering applications. Marine Geophysical Researches. 12, 153–168.

Schultheiss, P.J., McPhail, S.D., 1986. Direct indication of pore water advection from pore pressure measurements in the Madeira Abyssal Plain sediments. Nature 320, 348–350.

Schultheiss, P.J., Noel, M., 1987. Evidence of pore-water advection in the Madeira Abyssal Plain from pore-pressure and temperature measurements. In: Weaver, P.P.E., Thomson, J. (Eds.), Geology and Geochemistry of Abyssal Plains. Geological Society Special Publication, 31, pp. 113–129.

Simm, R.W., Weaver, P.P.E., Kidd, R.B., Jones, E.J.W., 1991. Late Quaternary mass movement on the lower continental rise and abyssal plain off Western Sahara. Sedimentology 38, 27–40.

Soderberg, L.O., 1962. Consolidation theory applied to foundation pile time effects. Géotechnique 12, 217–225.

Teide Group, 1997. Morphometric interpretation of the Northwest and southeast slopes of Tenerife, Canary Islands. Journal of Geophysical Research 102, 20 325–20 342.

Urgeles, R., Canals, M., Baraza, J., Alonso, B., Masson, D.G., 1997. The most recent megalandslides on the Canary Islands: the “El Golfo” debris avalanche and the Canary debris flow, west Hierro Island. Journal of Geophysical Research 102, 20 305–20 323.

Urgeles, R., Canals, M., Baraza, J., Alonso, B., 1998. Seismostratigraphy of the western flanks of Hierro and La Palma (Canary Islands): a record of the Canary Islands volcanism. Marine Geology 146, 225–241.

Urgeles, R., Masson, D.G., Canals, M., Watts, A.B., Le Bas, T., 2000. Recurrent giant landslides on the west flank of La Palma, Canary Islands. Journal of Geophysical Research 104(B11), 25331–25348.

Von Herzen, R.P., Cordery, M.J., Detrick, R.S., Fang, C., 1989. Heat flow and the thermal origin of hot spot swells: the Hawaiian Swell revisited. Journal of Geophysical Research 94, 13783–13799.

Wang, K., Davis, E.E., 1996. Theory for the propagation of tidally induced pore pressure variations in layered subseafloor formations. Journal of Geophysical Research 101, 11483–11495.

Wang, K., Davis, E.E., van der Kamp, G., 1998. Theory for the effects of free gas in subsea formations on tidal pore pressure variations and seafloor displacements. Journal of Geophysical Research 103, 12339–12353.

Watts, A.B., Masson, D.G., 1995. A giant landslide on the north flank of Tenerife, Canary Islands. Journal of Geophysical Research 100, 24487–24498.

Working Group 3, 1987. Fluid circulation in the crust and Global Geochemical Budget. Report of the Second Conference on Scientific Ocean Drilling (COSOD II), European Science Foundation, Strasbourg, France, pp. 67–86.